JCTC Journal of Chemical Theory and Computation

Article

pubs.acs.org/JCTC

Critical Importance of van der Waals Stabilization in Strongly Chemically Bonded Surfaces: Cu(110):O

J. Bamidele,[†] J. Brndiar,[‡] A. Gulans,[§] L. Kantorovich,[†] and I. Štich*[,‡]

[†]Department of Physics, King's College London, The Strand, London WC2R 2LS, United Kingdom,

[‡]Center for Computational Materials Science, Institute of Physics, Slovak Academy of Sciences, 84511 Bratislava, Slovakia

[§]COMP/Department of Applied Physics, Aalto University School of Science and Technology, P.O. Box 11100, FI-00076 Aalto, Finland

Supporting Information

ABSTRACT: We provide strong evidence that different reconstructed phases of the oxidized Cu(110) surface are stabilized by the van der Waals (vdW) interactions. These covalently bonded reconstructed surfaces feature templates that are an integral part of the surfaces and are bonded on the bare metal surface by a combination of chemical and physical bonding. The vdW stabilization in this class of systems affects predominantly the intertemplate Cu−O interactions in structures sparsely populated by these templates. The conventional dispersionless density functional theory (DFT) methods fail to model such systems. We find a failure to describe the thermodynamics of the different phases that are formed at different oxygen exposures and spurious minima on the potential energy surface of a diffusing surface adatom. To overcome these issues, we employ a range of different DFT methods that account for the missing vdW correlations. Surprisingly, despite vast conceptual differences in the different formulations of these methods, they yield physically identical results for the Cu(110):O surface phases, provided the massive screening effects in the metal are taken into account. Contrary, the vibrational contribution does not consistently stabilize the experimentally observed surface structures. The van der Waals surface stabilization, so far deemed to play only a minor role in hard-bonded surfaces, is suggested to be a more general key feature for this and other related surfaces.

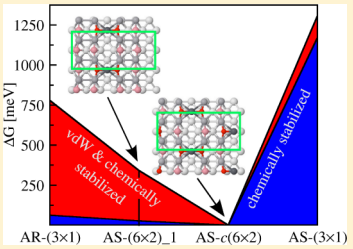

INTRODUCTION

van der Waals (vdW) interactions are routinely used in the description of sparse matter,[1] in studying interactions of closed-shell molecules and clusters among themselves[2−4] and with surfaces,[5−11] and in systems of biological relevance,[1] etc. While the coexistence of chemisorption and physisorption was reported in some of these systems,[9−11] all of them represent molecule−surface systems in a "conventional" adsorption regime. Contrary to these examples, some surfaces may serve as prototypical systems featuring well-pronounced and relatively strong chemical bonds, leading to what is typically called "hard" matter, and for them, vdW interactions are expected to play only a minor role, if any. Such a situation is analogical to strongly bonded hard bulk systems, where attempts to include vdW interactions typically worsen the results.[12] We report below on strongly bonded surfaces stabilized by vdW interactions. To the best of our knowledge, this is the first manifestation of a vdW stabilization of a surface via surface templates that are a part of the surface and are both chemisorbed and physisorbed on the metal substrate. The general mechanism of the combined chemical/physical surface stabilization, which is anticipated to be a more general phenomenon, is analyzed and demonstrated on a prototypical system, which is the oxidized Cu(110) surface.

Copper surfaces are important in their own right as industrial catalysts,[13−15] and surface oxidation is believed to play a crucial role in their catalytic activity.[16] In a recent study, it has also been proposed that oxidized copper surfaces could be employed as reference systems for chemical tip fingerprinting in atomic force microscopy techniques.[17]

The Cu(110) surface, with its major reconstructions,[18] is especially intricate. At low oxygen exposures, it forms a $p(2 \times 1)$ phase, while at higher exposures a $c(6 \times 2)$ phase is formed.[19] The $p(2 \times 1)$ phase, shown in Figure 1(a), has been studied extensively both experimentally and theoretically (see ref 18 and references therein), and its "added row" (AR) structure is generally accepted. The $c(6 \times 2)$ phase, Figure 1(b), has been studied considerably experimentally[19−21] but much less theoretically.[18] It has a "double AR" (or "added strand" (AS)) structure,[18] different from the single AR structure of the $p(2 \times 1)$ phase. Another key feature of the $c(6 \times 2)$ surface is the presence of additional copper atoms in every second row, known as "super" copper atoms,[19,20] which are bound between two oxygen atoms. As a result, the oxygen atoms bonded to them are raised slightly out of plane and are buckled in toward the super-Cu atoms, acquiring the names "high"[19] or "buckled"[20] oxygen atoms. These high oxygen atoms are bonded to the super-Cu atoms to form "super" CuO_2 molecules (or units) on the surface. The $c(6 \times 2)$ structure (henceforth referred to as AS-$c(6 \times 2)$) represents the tiling of the surface with Cu−O templates resulting in a $c(6 \times 2)$

Received: July 4, 2013

   dx.doi.org/10.1021/ct400813d | J. Chem. Theory Comput. XXXX, XXX, XXX−XXX

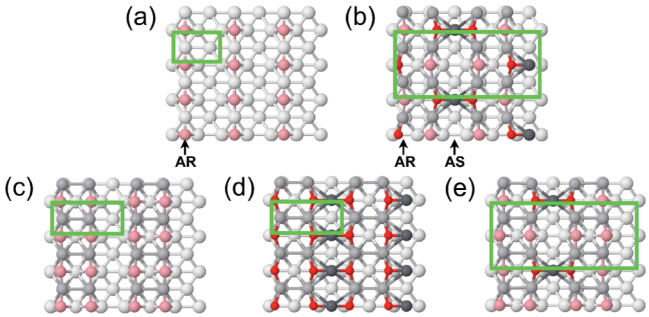

Figure 1. PBE-relaxed geometries (top view) of several models for the oxidized Cu(110) surface: (a) AR-$p(2 \times 1)$, (b) AS-$c(6 \times 2)$, (c) AR-(3×1), (d) AS-(3×1), and (e) AS-(6×2)_1. Silver, light gray, dark gray, pink, and red balls denote bulk Cu, Cu in ARs, super-Cu (Cu in ASs), O in ARs, and high O atoms, respectively. AS and AR are indicated by arrows, while green boxes indicate the periodic unit cells in each case.

arrangement of the "super" CuO_2 units. Examples of other possible variations of this building principle are depicted in Figure 1(b–e).

The AR-$p(2 \times 1)$ phase features a fairly simple structure free of additional templates and, hence, appears to be well described by standard DFT methods that predict its thermodynamic stability at low oxygen pressures. At the same time, however, the previous theoretical thermodynamic calculations[18] found the AS-$c(6 \times 2)$ reconstruction to be thermodynamically favorable at higher oxygen exposures from several other geometrically similar surface reconstructions by only a marginal ≈25 meV per surface unit cell. If this DFT modeling[18] was indeed correct, then one would expect to observe other reconstructions alongside the AS-$c(6 \times 2)$ phase, but only the latter has been experimentally reported at higher oxygen exposures before the bulk Cu_2O oxide forms. In addition, even for the AR-$p(2 \times 1)$ phase, we find a spurious minimum upon adsorption of additional Cu atoms, which has not been observed experimentally.[17,22]

We find that both failures are manifestations of the vdW bonding on these hard-bonded surfaces that can be fixed by addition of vdW correlations to the standard DFT surface description in a DFT–vdW model. However, the choice of the model is complicated as metals, especially copper, are known to exhibit massive screening and possibly also many-body effects[23,24] difficult to account for in a semi-infinite surface due to the long-range nature of the vdW interaction.[25] The vdW–DF2 method[26] and the Tkachenko–Scheffler many-body self-consistently screened (TS–SCS) theory[23,24,27] have been specifically developed to capture these screening and many-body features. Interestingly, they are based on completely opposite physical concepts: the TS–SCS method uses a localized picture and treats vdW effects as an add-on tool a posteriori, whereas the vdW–DF2 is based on a delocalized picture and is fully integrated into the DFT xc-functional. In addition to vdW–DF2 and TS–SCS, there have been more recent attempts to capture the effect of screening among fluctuating dipoles, see, for instance, ref 28. The effect of screening is treated in a completely different way in these approaches. Reference 28 introduces simple tools, such as the Thomas–Fermi-type of screening, while TS–SCS takes directly into account the long-range electrostatic screening among fluctuating dipoles by modeling the environment as a dipole field and solving the resulting classical electrodynamics SCS equations. However, the vdW–DF2 model builds in screening via the plasmon–pole model for the dielectric function. To the best of our knowledge, the TS–SCS technique has not been used on a surface as ye (see Supporting Information for more details). We use these and other DFT–vdW techniques to counteract the failures and, hence, to highlight the vdW stabilization on these otherwise hard-bonded surfaces.

METHODS

At variance with the previous calculations on these systems based on localized basis sets,[18] we use plane waves and the VASP code.[29] Within the standard DFT, electronic exchange–correlation interactions were described using the Perdew–Burke–Ernzerhof (PBE) generalized gradient approximation (GGA) functional,[30] but in addition, several different methods have been used as well to account for the vdW interaction as detailed below. All calculations were performed using projector augmented-wave pseudopotentials[31] and a plane wave cutoff of 500 eV; the k-point sampling was scaled from that of the bulk, which was done on a dense grid of ≈0.03 $Å^{-1}$ using the Methfessel and Paxton technique.[32] We used a slab model with a (6×2) unit cell and five atomic layers to represent the Cu(110) surface. In calculations on thermodynamic stability, over 30 models of the oxidized surface were tried differing in the structure of the upper reconstructed layer containing additional Cu and O atoms (Supporting Information).

In order to describe vdW interactions, we use primarily the TS–SCS[23] and vdW–DF2[26] theories. Three other theories have also been applied, namely, the ordinary Tkachenko–Scheffler (TS),[33] which takes into account chemistry and structure-related effects but disregards the screening effects, the optB86b reparametrization[6] (vdW–DF/optB86b) of the vdW–DF[34] theory proposed to improve lattice parameters and bulk moduli of solids, and the much simpler semi-empirical PBE–D2 method.[35] The more sophisticated PBE–D3 method[36] yields results in practical terms identical to PBE–D2 results, due to the fact that geometries and chemical environments similar to those encountered on our oxidized surfaces apparently were not included in the D3 interpolation database. While vdW–DF2 is fairly straightforward to apply to surface geometries, the same is not true for the TS-SCS approach; the application to a slab geometry led to uncontrolled results, presumably due to the long-range nature of the vdW interaction not being correctly accounted for. Therefore, we decided to use a finite disc geometry. This led to well converged results for TS–SCS C_6 dispersion coefficients for atoms in the first two layers at the center of the disc. The C_6 coefficients for central Cu atoms of other layers rapidly approach the bulk value of 103 au, which can be calculated separately in a fully periodic bulk geometry. More details and convergence tests for the TS–SCS method in the disc approximation to the slab model of the surface can be found in the Supporting Information. With this model, we captured the massive response screening effects on the C_6 coefficients but disregarded the three- and higher-order contributions. We note that, unlike the DFT–vdW^{surf} method,[37] the TS–SCS method is fully ab initio in the sense that no additional experimental input, such as dielectric function of the material, is needed. All C_6 coefficients, including the TS–SCS, were subsequently used in the electronic structure modeling and structural relaxation of the several most energetically favorable surface slab models. More technical details can be found in the Supporting Information.

dx.doi.org/10.1021/ct400813d | J. Chem. Theory Comput. XXXX, XXX, XXX–XXX

Table 1. Calculated Gibbs Free Energy Difference ΔG Relative to the AS-$c(6 \times 2)$ Phase without (with) Vibrational Contribution F^{vib}[a]

		ΔG (meV)						E_{DFT}	E_{DFT} E_{vdW}	
structure	n	PBE	TS	TS−SCS	vdW−DF2	optB86b	PBE−D2	PBE	TS−SCS	
AR-(3×1)	0	62 (214)	178	779 (434)	771 (530)	177 (−133)	582 (572)	–	–	–
AS-(6×2)_1	1	27 (148)	10	342 (318)	378 (529)	66 (45)	113 (251)	−35	−135	−306
AS-$c(6 \times 2)$	2	0	0	0	0	0	0	−31	−100	−289
AS-(3×1)	4	1171 (1086)	791	1306 (851)	1242 (994)	996 (738)	882 (786)	+277	+266	−137

[a]Here, E_{DFT} (E_{vdW}) denote PBE (vdW) contributions to the "adsorption" energy per super-Cu atom relative to the "bare" AR-(3×1) structure. n is the number of super-Cu atoms per 6×2 cell.

RESULTS AND DISCUSSION

We now turn to thermodynamics surface stability. The experimental conditions of high pressure and temperature of the oxygen gas environment being in thermal equilibrium with the copper surface are explicitly taken into account in DFT surface thermodynamics.[38] This is done using the chemical potential of oxygen, $\Delta\mu_O$ (defined *relative* to the half O_2 energy), which is a function of the molecular oxygen gas partial pressure, p_{O_2}, and temperature, T.[39] For the same slab size, the most stable surface structure has the lowest Gibbs free energy (GFE) difference

$$\Delta G^{slab}_{O/Cu} = G^{slab}_{O/Cu} - G^{slab}_{Cu} - \Delta N_{Cu}\mu_{Cu} - N_O\Delta\mu_O \quad (1)$$

for the given range of $\Delta\mu_O$ (p_{O_2} and/or T), relative to the bare surface. Here $G^{slab}_{O/Cu}$ and G^{slab}_{Cu} are the absolute GFEs of the surface under consideration and of the bare/clean surface, respectively. For our large cell sizes, we can neglect the pressure−volume term and approximate GFEs by total DFT energies. To facilitate the comparison, in all calculations, the same supercell was used based on the 6×2 extension. This allowed us to use the *relative* value ΔN_{Cu} for the number of Cu atoms in comparison with the bare Cu slab for all systems studied; N_O corresponds to the total number of oxygen atoms in the system. Therefore, the term $\Delta N_{Cu}\mu_{Cu}$ denotes the cost of trading ΔN_{Cu} copper atoms with the bulk, with the chemical potential μ_{Cu}, where the bulk and the surface copper atoms are assumed to be in thermodynamic equilibrium. Similarly, the last term in eq 1 denotes trading N_O oxygen atoms with the atmosphere saturated with molecular oxygen, also assumed to be in thermodynamic equilibrium with the surface. After initially screening with PBE, over 30 variations of the AS reconstruction of the oxidized Cu(110) surface as possible candidates at higher oxygen exposure (Supporting Information), four of those geometries, all corresponding to the lowest energy structures, Figure 1(b−e), were studied in more detail by including the vdW interaction and vibrational contributions.

We first focus on the relative Gibbs free energy differences and the effect of vdW stabilization as explained above. Vibrational contributions will be taken into account in the next step. PBE results (Table 1 and Supporting Information) show an excellent agreement with the study by Duan et al.;[18] although the AS-$c(6 \times 2)$ surface is indeed calculated as the most favorable in the appropriate window of $\Delta\mu_O$, there are several other structures very near in energy (Table 1). In fact, the AS-(6×2)_1 structure in Figure 1(e) differs only by 27 meV, which is well beyond the precision of DFT. More importantly, this tiny energy difference would predict coexistence of the two phases. Hence, conventional modeling without inclusion of dispersion interaction faces the fundamental problem of predicting several surfaces as being thermodynamically indistinguishable from the AS-$c(6 \times 2)$ surface; for effect of vibrations, see below.

DFT−vdW-based thermodynamics was modeled in different DFT−vdW approaches (see Methods section). The TS−SCS treatment is shown in Figure 2 and Table 1; the latter also summarizes the most important parameters obtained from the ordinary TS, vdW−DF2, and vdW−DF/optB86b treatments. One can see from Figure 2 that applying the TS−SCS method yields both that the AR-$p(2 \times 1)$ phase is the most favorable for a reasonable range of μ_O values, although this range of μ_O is significantly narrower than that calculated by the ordinary PBE (Supporting Information) and that the AS-$c(6 \times 2)$ surface is found to be the most favorable at larger values of μ_O. Most importantly, application of the TS−SCS DFT−vdW correction increases the energy separation between the AS-$c(6 \times 2)$ structure and the next one in energy, AS-(6×2)_1, by a factor of 14 relative to the PBE result, reaching 338 meV. Quite generally, all phases considered are significantly more separated after adding the vdW contribution, demonstrating the vdW stabilization of the $c(6 \times 2)$ phase. An alternative view on these results is depicted in Figure 3, which shows that the structures sparsely populated by the CuO_2 templates ($n = 1, 2$) experience most vdW stabilization, indicated by the almost horizontal line in treatment without the vdW stabilization and, hence, by degeneracy in energy. Contrary, in the densely populated structures ($n = 4$), the chemical stabilization (repulsion) is the decisive factor and results with and without vdW stabilization are similar. Perhaps the most stunning result is that the vdW

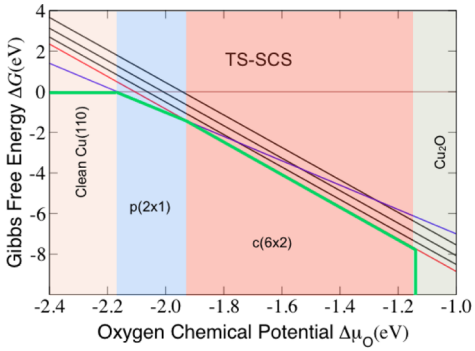

Figure 2. Gibbs free energy plots for the four most energetically favorable oxidized Cu(110) systems calculated using the TS−SCS method. The brown (horizontal), blue, and red lines correspond to the clean Cu(110) surface, AR-$p(2 \times 1)$, and AS-$c(6 \times 2)$ phases, respectively. The black lines correspond to the other three AS-$c(6 \times 2)$-like surfaces shown in Figure 1(c−e). The thick green line indicates the systems that are thermodynamically favorable for the given range of $\Delta\mu_O$.

dx.doi.org/10.1021/ct400813d | J. Chem. Theory Comput. XXXX, XXX, XXX−XXX

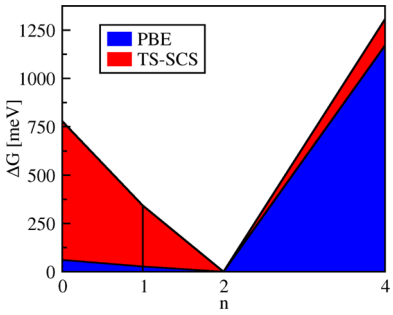

Figure 3. Graphical comparison of Gibbs free energy differences as a function of number of super-Cu atoms per 6 × 2 cell, *n*, relative to the AS-(6 × 2) phase, in dispersionless treatment (blue) and vdW-stabilized (TS−SCS) treatment (red).

description by the TS−SCS and vdW−DF2 methods yield almost identical results for the Cu(110):O surface phases with the largest difference of only ≈60 meV for the AS-(3 × 1). This result is important not only because the two theories approach vdW bonding from completely opposite stand-points (localized versus delocalized) but also because they use completely different models of exchange and short-range correlations (PBE[30] versus rPW86[26] and LDA[26]). This indirectly also indicates that the most important exchange−correlation effects for the surface region have been captured. Contrary to this, the TS yields PBE-type of results as does the vdW−DF/optB86b reparametrization that completely destroys the physical picture. This shows the delicacy that the correct treatment of vdW interactions in complex systems requires.

The energy balance between the chemical (DFT) and physical (vdW) interactions in different structures can also be compared by considering each phase as being obtained by "adsorbing" additional Cu atoms (with the "gas phase" energies μ_{Cu}) on the "bare" AR-(3 × 1) phase (Figure 1(c)). In the last two columns of Table 1, the relative (with respect to the "bare" phase) chemical (PBE) and physical (vdW) contributions to the total energies of the three structures are given, calculated per super-Cu atom in the TS−SCS approach as an example. The AS-(6 × 2)_1 structure, which is the nearest contender to the AS-*c*(6 × 2) phase, is seen to lie somewhat lower in energy due to DFT *and* vdW contributions upon the addition of a single super-Cu atom. Adding two atoms (yielding the AS-*c*(6 × 2) phase) results in a slight reduction of both the chemical and the vdW energies; overall, however, this phase becomes more favorable as both contributions are doubled. Adding four super-Cu atoms to construct the AS-(3 × 1) structure results in significant chemical repulsion between CuO_2 units and also in a noticeable decrease in the vdW energy (per added atom) as compared with the AS-*c*(6 × 2) system. This analysis indicates a delicate balance of the chemical and physical interactions in this system that eventually favors the AS-*c*(6 × 2) phase observed experimentally. From this analysis, it follows that the vdW interaction affects mainly the intertemplate Cu−O interaction of an otherwise very strongly surface-bonded CuO_2 template. Incidentally, as shown in Table 1, inclusion of dispersion interactions increases also the chemical bonding (E_{DFT}) within the CuO_2 template.

In order to better understand the complexities of vdW bonding in our system, in Figure 4 we show the variation of the C_6 coefficients for the AS-*c*(6 × 2) phase in various approaches. In the TS−SCS calculations the copper C_6 coefficients are reduced by a factor of ≈2.5 with respect to unscreened TS

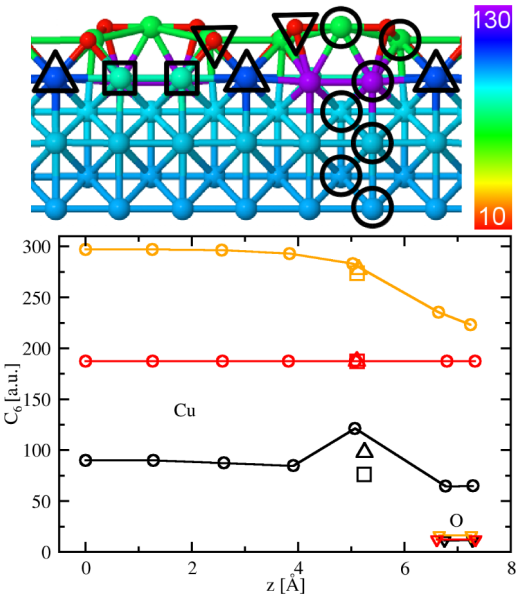

Figure 4. Calculated distribution of C_6 coefficients on atoms of the AS-*c*(6 × 2) surface calculated with TS−SCS (black), PBE-D2 (red), and ordinary TS (yellow) methods. The variation of the values of the C_6 coefficients in the TS−SCS treatment on Cu and O atoms is shown as a function of their position in the slab as indicated by symbols detailed in the upper panel. z = 0.0 Å corresponds to the bottom of the slab.

values, and there is an additional variation by a factor of ≈2 due to structure and chemistry. Contrary to this, the TS approach, which lacks screening, captures well the structure/chemistry-related reduction as going from the bulk to the surface but fails to capture the massive reduction due to screening, while PBE−D2 implements fixed values somewhere in between without any variation with screening, structure, or chemistry. All three approaches however yield similar and significantly smaller oxygen dispersion coefficients.

As a next step, we have included the contribution to the Gibbs free energy due to vibrations, F^{vib} using the frozen phonon method and the quasi-harmonic approximation.[40] As can be seen in Table 1, the effect of adding F^{vib} is less clear-cut and strongly dependent on the form of the vdW contribution. In the cases of TS−SCS (vdW−DF/optB86b), inclusion of vibrations resulted in slight *worsening* (*reversal*) in the relative stability of the AS-*c*(6 × 2) phase with respect to its major competitor AS-(6 × 2)_1; in the cases of PBE and vdW−DF2, accounting for vibrations widens the gap between these two phases. In either case, the energy difference between the AS-*c*(6 × 2) and other phases remains significant enough to claim with certainty that this phase is the most favorable.

From these results, one could naively conclude that vibrations alone, i.e., without considering the vdW correlations, may lead to stabilization of the AS-*c*(6 × 2) structure over the other contenders (see PBE results with vibrations in Table 1). However, pure vibrational stabilization on the incorrect ground state potential energy surface (PES), i.e., yielding incorrect ordering without vibrations, is only accidental. For instance, substituting the short-range PBE correlations with PW91 correlations[41] stabilizes the AS-*c*(6 × 2)_1 structure without vibrations and AS-(3 × 1) with vibrations. Hence, vibrations alone are *not* sufficient.

dx.doi.org/10.1021/ct400813d | J. Chem. Theory Comput. XXXX, XXX, XXX−XXX

The CuO_2 templates on the AS-$c(6 \times 2)$ phase exhibited significant vdW stabilization. We show now that the same remains valid for a simpler problem of *diffusion* of a Cu atom on the AR-$p(2 \times 1)$ surface between two equivalent "super"-Cu positions along an AS row. The potential energy surface for a super-Cu atom is shown in Figure 5. Two minima at the beginning and the end of the trajectory correspond to the Cu atom in the "super"-Cu position bonded to two adjacent oxygen atoms, and there is also a minimum midway between the two minima with the Cu atom bonded to its nearest copper atoms. The PBE calculated midway minimum is by 50 meV lower in energy than the two minima at the "super" positions. This would mean that deposited Cu atoms would preferentially be observed on the AS rows between the nearest Cu atoms and *not* between oxygen atoms. However, experiments strongly suggest that the Cu-bonded minimum is a PBE artifact, leading to a qualitatively incorrect PES, as Cu atoms deposited on the AR-$p(2 \times 1)$ surface are experimentally found only in oxygen-bonded "super" positions.[17,22] As shown in Figure 5 and Table 2, the spurious minimum is significantly lifted in energy by adding vdW correlations leading to the PES with Cu atoms favored to occupy the "super"-Cu positions, in qualitative agreement with experimental observations. The exception being the vdW−DF/optB86b that fails to correct the spurious PBE minimum significantly leading essentially to a PBE-type of PES. TS−SCS and vdW−DF2 grossly reduce the stability of the spurious minimum, yielding qualitatively correct and similar results, and this is also the case for other methods (TS and PBE−D2), albeit with more modest corrections to PBE.

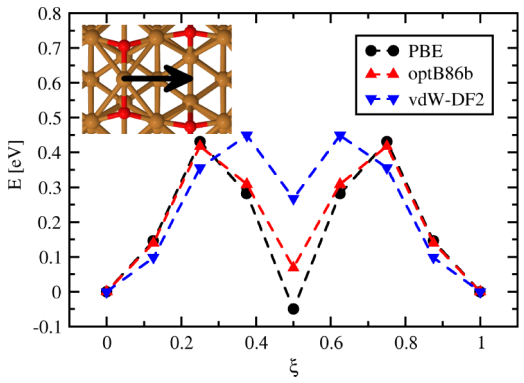

Figure 5. Potential energy surface for a super-Cu atom on the AR-$p(2 \times 1)$ phase moving along the [110] direction, see inset, in different DFT−vdW approaches.

Table 2. Energy Difference ΔE between the Global and Local Minima for Super-Cu Atom Moving along the [110] Direction on AR-$p(2 \times 1)$ Surface in Different DFT−vdW Approaches

method	PBE	TS	TS−SCS	vdW−DF2	optB86b	PBE−D2
ΔE (meV)	−50	206	458	268	69	195

SUMMARY AND CONCLUSIONS

To summarize, we report on a class of oxidized Cu(110) surfaces that are stabilized by vdW interactions. Such a stabilization is signaled by severe failures of conventional DFT methods, namely, spurious minima on the PES for super-Cu atoms on the AR-$p(2 \times 1)$ phase and the thermodynamic stability of the concurrent high-oxygen exposure phases. Our systems do *not* represent conventional molecule−surface systems in adsorption regime but are rather results of their reconstructions with vdW-stabilized templates (CuO_2 molecules) that are strongly surface bonded via oxygens and are part of the surface. The vdW stabilization proceeds mainly via intra-template modification of the super-Cu atoms. The missing nonlocal correlation effects have been added in a number of different approximate models. Surprisingly, both the Tkachenko−Scheffler SCS and the vdW−DF2 theories, built on completely opposite philosophies, yield identical results for the Cu(110):0 surface phases, strongly suggesting that the most important correlation effects in this system have indeed been included. This requires the massive screening effects in copper to be captured, which is the case for both methods. While these methods correctly account for the correlations on the surface, bulk calculations indicate that the same methods may *not* be optimal for the bulk (Supporting Information). The subtlety of the effect is demonstrated by attempts to correct the picture by using functionals that describe the bulk well, such as the optB86b reparametrization of the vdW−DF theory, but which completely destroy the description of the surface. Contrary to vdW stabilization, the vibrational contribution does not consistently stabilize the experimentally observed surface structures.

We are convinced that the effect we observe is not limited to only the oxidized Cu(110) surface and will be seen on a number of other surface systems with motifs showing joint chemisorbed and physisorbed features. For example, oxidized Cu(100),[18] Ag(100),[42] Ag(110),[43] Ag(111),[44] Ni(110),[45] and Au(110),[46] which all have either a missing row reconstruction with possible presence of super metal atoms or distinct and different arrangements of metal and oxygen atoms, are the most obvious candidates. On the basis of our results, we believe that vdW stabilization is an essential ingredient in this class of systems and of any computational scheme to be used in studying structure and stability of these and similar surfaces.

ASSOCIATED CONTENT

Supporting Information

Details of all the structures considered and determination of dispersion coefficients in the TS-SCS method, as well as a complete account of results obtained by all methods considered. This material is available free of charge via the Internet at http://pubs.acs.org.

AUTHOR INFORMATION

Corresponding Author

*E-mail: ivan.stich@savba.sk.

Notes

The authors declare no competing financial interest.

ACKNOWLEDGMENTS

Financial support from the U.K. Engineering and Physical Sciences Research Council (EPSRC), APVV (APVV-0207-11), and VEGA (2/0007/12) are greatly appreciated. We also acknowledge the support from the King's College London HPC Facility managed by Dr. Alessio Comisso and Computing Centre of the Slovak Academy of Sciences and use of the supercomputing infrastructure funded by the ERDF, projects ITMS 26230120002 and 26210120002. We thank the Material

Chemistry consortium for the computer time allocation at the HECToR UK National facility.

REFERENCES

(1) Parsegian, V. A. *Van der Waals Forces: A Handbook for Biologists, Chemists, Engineers, and Physicists*; Cambridge University Press: England, 2005.

(2) Hobza, P.; Šponer, J. Toward true DNA base-stacking energies: MP2, CCSD(T), and complete basis set calculations. *J. Am. Chem. Soc.* **2002**, *124*, 11802−11808.

(3) Jurečka, P.; Šponer, J.; Černý, J.; Hobza, P. Benchmark database of accurate (MP2 and CCSD(T) complete basis set limit) interaction energies of small model. *Phys. Chem. Chem. Phys.* **2006**, *8*, 1985−1993.

(4) Brndiar, J.; Štich, I. van der Waals interaction energies of small fragments of P, As, Sb, S, Se, and Te: Comparison of complete basis set limit CCSD(T) and DFT with approximate dispersion. *J. Chem. Theor. Comput.* **2012**, *8*, 2301−2309.

(5) Chakarova-Käck, S. D.; Schröder, E.; Lundqvist, B. I.; Langreth, D. C. Application of van der Waals density functional to an extended system: Adsorption of benzene and naphthalene on graphite. *Phys. Rev. Lett.* **2006**, *96*, 146107.

(6) Klimes, J.; Bowler, D. R.; Michaelides, A. Chemical accuracy for the van der waals density functional. *J. Phys.: Condens. Matter* **2010**, *22*, 022201.

(7) Mura, M.; Gulans, A.; Thonhauser, T.; Kantorovich, L. Role of van der waals interaction in forming molecule-metal junctions: flat organic molecules on the au(111) surface. *Phys. Chem. Chem. Phys.* **2010**, *12*, 4759−4767.

(8) Moses, P. G.; Mortensen, J. J.; Lundqvist, B. I.; Nørskov, J. K. Density functional study of the adsorption and van der Waals binding of aromatic and conjugated compounds on the basal plane of MoS2. *J. Chem. Phys.* **2009**, *130*, 104709.

(9) Atodiresei, N.; Caciuc, V.; Lazič, P.; Blügel, S. Chemical versus van der Waals Interaction: The role of the heteroatom in the flat absorption of aromatic molecules C6H6, C5NH5, and C4N2H4 on the Cu(110) Surface. *Phys. Rev. Lett.* **2009**, *102*, 136809.

(10) Liu, W.; Carrasco, J.; Santra, B.; Michaelides, A.; Scheffler, M.; Tkatchenko, A. Benzene adsorbed on metals: Concerted effect of covalency and van der Waals bonding. *Phys. Rev. B* **2013**, *86*, 245405.

(11) Lee, K.; Berland, K.; Yoon, M.; Andersson, S.; Schröder, E.; Hyldgaard, P.; Lundqvist, B. I. Benchmarking van der Waals density functionals with experimental data: potential-energy curves for H-2 molecules on Cu(111), (100) and (110) surfaces. *J. Phys.: Condens. Matter* **2012**, *24*, 424213.

(12) Klimes, J.; Bowler, D. R.; Michaelides, A. Van der Waals density functionals applied to solids. *Phys. Rev. B* **2011**, *83*, 195131.

(13) Guerrero-Ruiz, A.; Rodrigues-Ramos, I.; Fierro, J. L. G. Dehydrogenation of methanol to methyl formate over supported copper catalysts. *Appl. Catal.* **1991**, *72*, 119−137.

(14) Louis-Rose, I.; Méthivier, C.; Pradier, C.-M. Oxidation of NH_3 on polycrystalline copper and Cu(110): A combined FT-IRAS and kinetics investigation. *Catal. Today* **2003**, *85*, 267−278.

(15) Mayer, R. W.; Hävecker, M.; Knop-Gericke, A.; Schlögl, R. Investigation of Amonia oxidation over copper with in situ NEXAFS in the soft X-ray range: Influence of pressure on the catalyst performance. *Catal. Lett.* **2001**, *74*, 115−119.

(16) Stampfl, C. Surface processes and phase transittions from ab initio atomistic thermodynamics and statistical mechanics. *Catal. Today* **2005**, *105*, 17−35.

(17) Bamidele, J.; Kinoshita, Y.; Turanský, R.; Lee, S. H.; Naitoh, Y.; Li, Y. J.; Sugawara, Y.; Štich, I.; Kantorovich, L. Chemical tip fingerprinting in scanning probe microscopy of oxidized Cu(110) surface. *Phys. Rev. B* **2012**, *86*, 155422.

(18) Duan, X.; Warschkow, O.; Soon, A.; Delley, B.; Stampfl, C. Density functional study of oxygen on Cu(100) and Cu(110) surfaces. *Phys. Rev. B* **2010**, *81*, 075430.

(19) Kishimoto, S.; Kageshima, M.; Naitoh, Y.; Li, Y. J.; Sugawara, Y. Study of oxidized Cu(110) surface using noncontact atomic force microscopy. *Surf. Sci.* **2008**, *602*, 2175−2182.

(20) Feidenhanšl, R.; Grey, F.; Nielsen, M.; Besenbacher, F.; Jensen, F.; Laegsgaard, E.; Stensgaard, I.; Jacobsen, K. W.; Nørskov, J. K.; Johnson, R. L. Oxygen chemisorption on Cu(110): A model for the c(6 × 2) structure. *Phys. Rev. Lett.* **1990**, *65*, 2027−2030.

(21) Liu, W.; Wong, K. C.; Mitchell, K. A. R. Structural details for the Cu(110)−c(6 × 2)−O surface determined by tensor LEED. *Surf. Sci.* **1995**, *339*, 151−158.

(22) Sugawara, Y. Private communication.

(23) Tkatchenko, A.; DiStasio, R. A.; Car, R.; Scheffler, M. Accurate and efficient method for many-body van der Waals interactions. *Phys. Rev. Lett.* **2012**, *108*, 236402.

(24) Tkatchenko, A.; Ambrosetti, A.; DiStasio, R. A. Interatomic methods for the dispersion energy derived from the adiabatic connection fluctuation-dissipation theorem. *J. Chem. Phys.* **2013**, *138*.

(25) Hanke, F.; Dyer, M. S.; Björk, J.; Persson, M. Structure and stability of weakly chemisorbed ethene adsorbed on low-index Cu surfaces: performance of density functionals with van der Waals interactions. *J. Phys.: Condens. Matter* **2012**, *24*, 424217.

(26) Lee, K.; Murray, E. D.; Kong, L.; Lundqvist, B. I.; Langreth, D. C. Higher-accuracy van der Waals density functional,. *Phys. Rev. B* **2010**, *82*, 081101(R).

(27) Bučko, T.; Lebégue, S.; Hafner, J.; Ángyán, J. G. Tkatchenko−Scheffler van der Waals correction method with and without self-consistent screening applied to solids. *Phys. Rev. B* **2013**, *87*, 064110.

(28) Silvestrelli, P. L.; Alberto Ambrosetti, A. Inclusion of screening effects in the van der Waals corrected DFT simulation of adsorption processes on metal surfaces. *Phys. Rev. B* **2013**, *87*, 075401.

(29) Kresse, G.; Furthmüller, J. Efficient iterative schemes for ab initio total-energy calculations using a plane-wave basis set. *Phys. Rev. B* **1996**, *54*, 11169−11186.

(30) Perdew, J. P.; Burke, K.; Ernzerhof, M. Generalized gradient approximation made simple. *Phys. Rev. Lett.* **1996**, *77*, 3865−3868.

(31) Blöchl, P. E. Projector augmented-wave method. *Phys. Rev. B* **1994**, *50*, 17953−17979.

(32) Methfessel, M.; Paxton, A. T. High-precision sampling for Brillouin-zone integration in metals. *Phys. Rev. B* **1989**, *40*, 3616−3621.

(33) Tkatchenko, A.; Scheffler, M. Accurate molecular van der Waals interactions from ground-state electron density and free-atom reference data. *Phys. Rev. Lett.* **2009**, *102*, 073005.

(34) Dion, M.; Rydberg, H.; Schröder, E.; Langreth, D. C.; Lundqvist, B. I. van der Waals density functional for general geometries. *Phys. Rev. Lett.* **2004**, *92*, 246401.

(35) Grimme, S. Semiempirical gga-type density functional constructed with a long-range dispersion correction. *J. Comput. Chem.* **2006**, *27*, 1787−1799.

(36) Grimme, S.; Anony, J.; Ehrlich, S.; Krieg, H. A consistent and accurate ab initio parametrization of density functional dispersion correction (DFT-D) for the 94 elements H-Pu. *J. Chem. Phys.* **2010**, *132*, 154104.

(37) Ruiz, V. G.; Liu, W.; Zojer, E.; Scheffler, M.; Tkatchenko, A. Density-functional theory with screened van der Waals interactions for the modeling of hybrid inorganic−organic systems. *Phys. Rev. Lett.* **2012**, *108*, 146103.

(38) Li, W. X.; Stampfl, C.; Scheffler, M. Insights into the function of silver as an oxidation catalyst by ab initio atomistic thermodynamics. *Phys. Rev. B* **2003**, *68*, 165412.

(39) Reuter, K.; Scheffler, M. Composition and structure of the RuO_2(110) surface in an O_2 and CO environment: Implications for the catalytic formation of CO_2. *Phys. Rev. B* **2003**, *68*, 045407.

(40) Kantorovich, L. *Quantum Theory of the Solid State: An Introduction*; Kluwer Academic Publishers: Dordrecht, 2004; Chapter 4.5.4.

(41) Perdew, J. P.; Y. Wang, Y. Accurate and simple analytic representation of the electron−gas correlation energy. *Phys. Rev. B* **1992**, *45*, 13244−13249.

(42) Bonini, N.; Kokalj, A.; Corso, A. D.; de, G. S.; Baroni, S. Structure and dynamics of the missing-row reconstruction on O/Cu(001) and O/Ag(001). *Surf. Sci.* **2006**, *600*, 5074−5079.

(43) Nakagoe, O.; Watanabe, K.; Takagi, N.; Matsumoto, Y. In situ observation of CO oxidation on Ag(110)(2 × 1)−O by scanning tunneling microscopy: Structural fluctuation and catalytic activity. *J. Phys. Chem. B* **2005**, *109*, 14536−14543.
(44) Knudsen, J.; Martin, N. M.; Grånäs, E.; Blomberg, S.; Gustafson, J.; Andersen, J. N.; Lundgren, E.; Klacar, S.; Hellman, A.; Grönbeck, H. Carbonate formation on p(4 × 4)−O/Ag(111). *Phys. Rev. B* **2011**, *84*, 115430.
(45) Ruan, L.; Besenbacher, F.; Stensgaard, I.; Laegsgaard, E. Atom-resolved discrimination of chemically different elements on metal-surfaces. *Phys. Rev. Lett.* **1993**, *70*, 4079−4082.
(46) Shi, H.; Stampfl, C. Shape and surface structure of gold nanoparticles under oxidizing conditions. *Phys. Rev. B* **2008**, *77*, 094127.